Single to Multiquasiparticle Excitations in the Itinerant Helical Magnet $CeRhIn_5$

C. Stock,[1] J. A. Rodriguez-Rivera,[2,3] K. Schmalzl,[4] E. E. Rodriguez,[5] A. Stunault,[6] and C. Petrovic[7]
[1]School of Physics and Astronomy and Centre for Science at Extreme Conditions, University of Edinburgh, Edinburgh EH9 3FD, United Kingdom
[2]NIST Center for Neutron Research, National Institute of Standards and Technology, 100 Bureau Drive, Gaithersburg, Maryland 20899, USA
[3]Department of Materials Science, University of Maryland, College Park, Maryland 20742, USA
[4]Julich Centre for Neutron Science, Forschungszentrum Julich GmbH, Outstation at Institut Laue-Langevin, Boite Postale 156, 38042 Grenoble Cedex 9, France
[5]Department of Chemistry of Biochemistry, University of Maryland, College Park, Maryland 20742, USA
[6]Institute Laue-Langevin, 71 Avenue des Martyrs, CS 20156, F-38042, Grenoble Cedex 9, France
[7]Department of Physics, Brookhaven National Laboratory, Upton, New York 11973, USA
(Received 11 August 2014; revised manuscript received 9 March 2015; published 19 June 2015)

$CeRhIn_5$ is an itinerant magnet where the Ce^{3+} spins order in a simple helical phase. We investigate the spin excitations and observe sharp spin waves parameterized by a nearest-neighbor exchange, $J_{RKKY} = 0.88 \pm 0.05$ meV. At higher energies, the spin fluctuations are heavily damped, where single-quasiparticle excitations are replaced by a momentum- and energy-broadened continuum constrained by kinematics of energy and momentum conservation. The delicate energy balance between localized and itinerant characters results in the breakdown of the single-quasiparticle picture in $CeRhIn_5$.

DOI: 10.1103/PhysRevLett.114.247005 PACS numbers: 74.70.Tx, 75.40.Gb, 75.50.Cc

The noninteracting quasiparticle description of excitations is fundamental to condensed matter physics and the understanding of low-energy fluctuations. However, interacting quasiparticle states have recently been recognized as important for the understanding of anomalous phases. For example, composite states including resonating valence bond states [1], Zhang-Rice singlets [2], or spinon-holons in the pseudogap [3], have been suggested to be fundamental to superconductivity, frustrated magnetism, and even quantum criticality [4–6]. We use neutron scattering to measure the breakdown of the single-quasiparticle description of the spin excitations in a helical itinerant heavy fermion magnet.

$CeRhIn_5$ is a heavy fermion metal, part of the $CeTIn_5$ (T = Rh, Ir, and Co) series that displays an interplay between localized antiferromagnetism and superconductivity [7–10]. The presence of two-dimensional layers of Ce^{3+} ions connects the physics of these systems with other unconventional superconductors, as in the cuprates [11–15] or iron-based pnictide or chalcogenide superconductors [16–18]. $CeRhIn_5$ magnetically orders at $T_N = 3.8$ K [19–21] and enters an unconventional superconducting phase that can be accessed under hydrostatic pressures or temperatures below ~75 mK [22–26].

$CeRhIn_5$ is isostructural with $CeCoIn_5$, which is superconducting at ambient pressures with $T_c = 2.3$ K [14]. The order parameter of the superconducting phase has a d-wave symmetry with nodes in the ab plane [27,28]. Magnetism and superconductivity are strongly coupled, as evidenced by neutron scattering measurements reporting a doublet spin-resonance peak connected with superconductivity and indicating an order parameter that changes sign, consistent with d-wave symmetry [29–31]. At high magnetic fields near H_{c2}, an unusual magnetic Q phase has been reported to exist in a narrow field region, further confirming the interplay between superconductivity and the localized magnetism [32,33].

Neutron measurements were performed at NIST (Gaithersburg, USA) using MACS [34] and at the ILL (Grenoble, France) using the IN12 spectrometer and the D23 and D3 diffractometers. The HHL-aligned sample was prepared using self-flux method [14]. To correct for the large neutron absorption [35,36], a finite element analysis has been done. Further details are provided in the Supplemental Material [37].

We first review the low-temperature magnetic structure using spherical polarimetry [38–40]. As found in the pioneering work by Bao *et al.* [19], the magnetic structure [Fig. 1(a)] is characterized by an incommensurate Bragg peak $\mathbf{Q} = (0.5, 0.5, 0.297)$. Figure 1(b) plots the results of our polarized diffraction experiment confirming this with measured (P_{measured}) against calculated ($P_{\text{calculated}}$) polarization matrix elements, assuming a perfect $a-b$ helix with the moment defined by $\mathbf{M} = \mathbf{M}_a + i\mathbf{M}_b$ (with $|\mathbf{M_a}| = |\mathbf{M_b}|$) and a propagation vector along c. Expressions for the matrix elements are given in the Supplemental Material [37]. Confirming the helical magnetism, a volume imbalance between the two chiral domains $\eta = 0.68 \pm 0.05$ was needed to account for off-diagonal matrix elements. Unpolarized diffraction measures the ordered magnetic

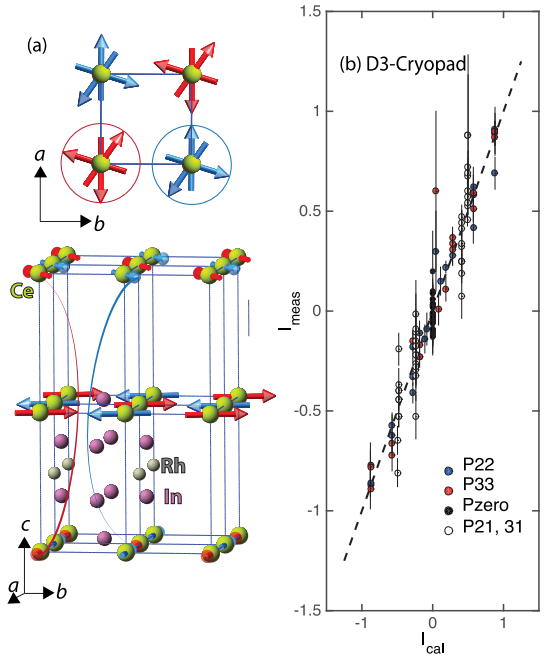

FIG. 1 (color online). The magnetic structure of $CeRhIn_5$ investigated using spherical polarimetry. (a) An illustration of the magnetic structure. (b) A plot of the polarization matrix elements P_{measured} vs $P_{\text{calculated}}$ based upon the isotropic helical model shown in (a).

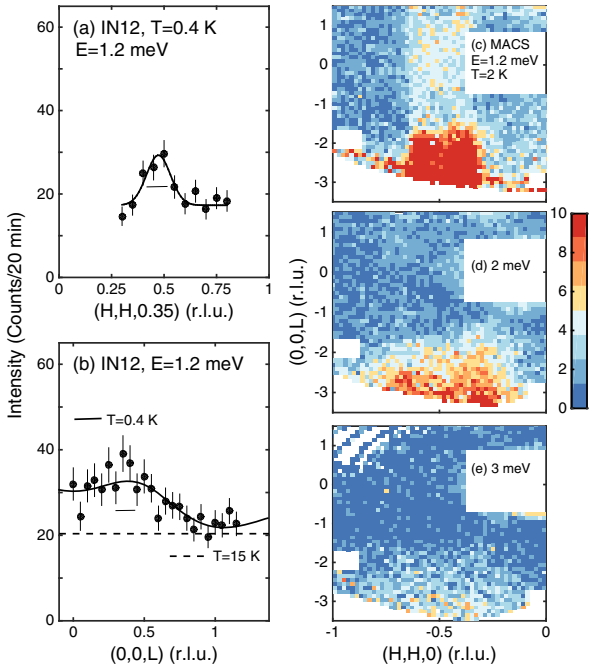

FIG. 2 (color online). Constant energy scans taken on IN12 and MACS in the antiferromagnetic phase. (a)–(b) illustrate fluctuations polarized along c with the horizontal bar being the spectrometer resolution. (c)–(e) show constant energy slices showing the energy dependence of the spin fluctuations. Fluctuations at large L characteristic of predominately $a-b$-plane polarized fluctuations are present to high-energy transfers.

moment to be $0.34 \pm 0.05\ \mu_B$ per cerium ion, consistent with expectations from crystal field theory [41]. The derived magnetic structure and symmetry analysis is also consistent with predictions from Landau theory for the phase transition, as outlined in the Supplemental Material [37,42,43].

We now discuss the inelastic scattering probing the dynamics. Figure 2 illustrates a summary of constant energy scans. Figure 2(a) shows a momentum scan along [110], finding the scattering to be peaked at (0.5, 0.5), indicating antiferromagnetic correlations within the $a-b$ plane. Figure 2(b) shows a scan along the [001] direction (corrected for absorption), finding momentum broadened correlations which decay rapidly with L. The solid line is a fit to $I(\mathbf{Q}) \propto f(Q)^2 \times [1-(\hat{\mathbf{Q}}\cdot\hat{\mathbf{c}})^2]\sinh(c/\xi_c)/[\cosh(c/\xi_c)+\cos(\mathbf{Q}\cdot\mathbf{c})]$, which represents short-range antiferromagnetically correlated Ce^{3+} moments polarized along c with a dynamic correlation length ξ_c. $f(Q)^2$ is the magnetic form factor [44]. The dynamic correlation length was derived to be $\xi_c = 3.1 \pm 0.7$ Å, indicating little coupling between the Ce^{3+} layers. The strong decrease in intensity with momentum transfer along L illustrates that these fluctuations are predominately out of the $a-b$ plane (c-axis polarized) and, hence, are referred to here as out-of-plane fluctuations (see Supplemental Material [37]).

Figures 2(c)–2(e) illustrate full constant energy maps taken on MACS at energy transfers of 1.2–3 meV. Figure 2(c) illustrates that, in addition to the magnetic scattering near $L = 0$ from the out-of-plane fluctuations, strong scattering is also present at large L, indicative of fluctuations predominately polarized within the $a-b$ plane; these are here referred to as in-plane fluctuations. We note that the energy transfer is significantly less than the first crystal field excitation at ~7–9 meV, indicating that the transition results from excitations within the lowest energy Ce^{3+} doublet [45,46]. The correlated scattering is present at higher energies as evidenced by similar scans in Figs. 2(d) and 2(e).

We now discuss the energy dependence. Constant energy and momentum cuts are shown in Figs. 3(a)–3(c) and Figs. 3(d)–3(f), respectively. As seen in both types of cuts, at low energies the magnetic dynamics are described by two components—one that is sharp and resolution limited in energy and momentum, and the second, of higher energy, that is broadened in both momentum and energy.

Figure 4(c) displays a constant-Q slice (integrating over $L = [-1.5, -4]$) sensitive to the predominately in-plane scattering. When all of the scattering is integrated over the magnetic Brillouin zone, the total spectral weight (accounting for absorption) is estimated at $2.0 \pm 0.5\ \mu_B^2$, agreeing with expectations from single-ion crystal field analysis (see Supplemental Material [37]). Both components need to be considered to satisfy sum rules and obtain all of the required dynamic spectral weight.

Neutron scattering is constrained by strict selection rules, with the scattering process having $\Delta S_z = \pm 1$ or 0.

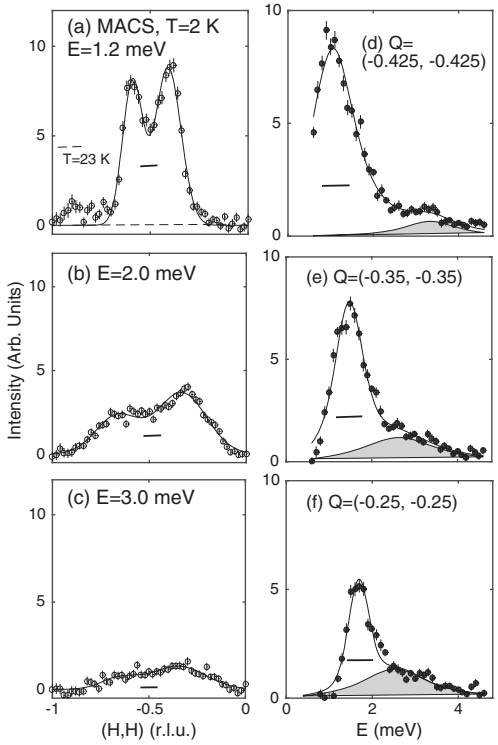

FIG. 3. Constant energy [(a)–(c)] and Q [(d)–(f)] cuts integrating over $L = [-4, -1.25]$ sensitive to predominately in-plane fluctuations. The solid lines in (a)–(c) are to Gaussians displaced from the commensurate $(\frac{1}{2}, \frac{1}{2})$ position. The solid lines in (d)–(f) are fits to damped harmonic oscillators. The shaded region is the broad heavily damped component. (d)–(f) are integrated over $\pm(0.025, 0.025)$. The solid bars represent the experimental resolution.

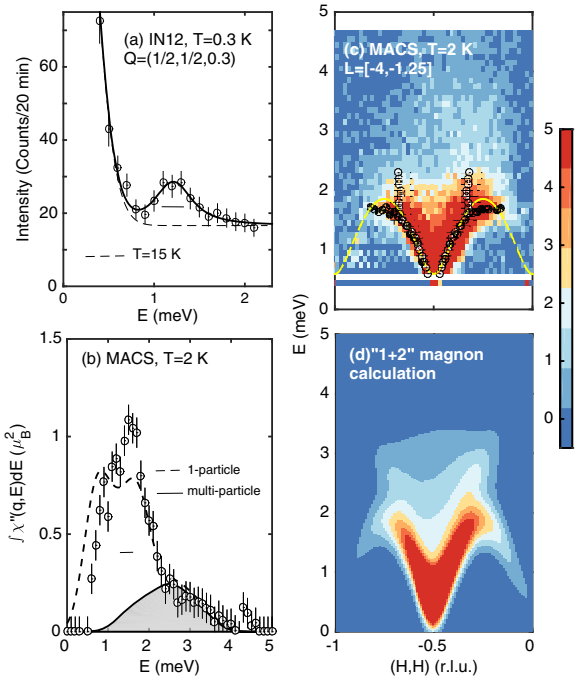

FIG. 4 (color online). Constant-Q scans taken on IN12 and MACS. (a) Illustrates the energy dependence of the c-axis-polarized spin fluctuations. (b) The momentum integrated spectral weight as a function of energy. (c) A constant-Q slice taken on MACS (integrating $L = [-4, -1.25]$), where the solid points are fits to constant-Q scans and the open circles fits to constant energy. A continuum of scattering is present above the top of the 1-magnon band. (d) A calculation considering the parameterization in single ("1") and multiparticle ("2") states with the $\vec{Q}$ integrated intensities plotted in (b).

Transverse spin excitations derive from harmonic theory and can be written as single-quasiparticle or -magnon excitations, which are long lived in a magnetically ordered structure with resolution-limited inelastic peaks. Other anharmonic processes can occur, including scattering from two magnons with opposite sign (i.e., the $\Delta S_z = 0$ process), provided that there is an interaction term between the single-magnon quasiparticles in the Hamiltonian. For collinear magnets, such terms are predicted to be weak from symmetry considerations; however, for a noncollinear magnet, such as a magnetic spiral or helix, such constraints are relaxed [47,48]. This additional cross section in the neutron response is constrained by momentum- and energy-conserving processes, and is possible over a wide range in energy and momentum which is determined by the single-magnon dispersion. Analogous classic examples of this cross section are found in model insulating low-spin chains [49–55]. We now investigate whether the two-component line shape found here can be understood in terms of a single- and multiparticle parameterization.

We first consider the low-energy component of the cross section that is also resolution limited in energy. Magnetic excitations for a planar helical magnet with a characteristic wave vector $\vec{q}_c$ are described by three modes, with $\vec{Q} = \pm\vec{q}_c$ being in-plane modes and a commensurate mode describing out-of-plane fluctuations [56–59].

Figure 4(a) shows a constant $\vec{Q} = (0.5, 0.5, 0.3)$ scan that is derived to have a strong c-axis-polarized character. An antisymmetric Lorentzian fit gives a peak energy position of $\hbar\Omega = 1.21 \pm 0.06$ meV and linewidth (half-width) of $\hbar\Gamma = 0.22 \pm 0.14$ meV. The out-of-plane fluctuations are, therefore, gapped as well as weakly dispersing.

To extract a dispersion and, hence, an estimate for the in-plane exchange interaction, we have fit constant energy scans [examples shown in Figs. 3(a)–3(c)] to Gaussians symmetrically displaced from the $\vec{Q} = (\frac{1}{2}, \frac{1}{2})$ and illustrated by the open circles in Fig. 4(c). The constant energy fits show dispersing excitations at wave vectors close to $(\frac{1}{2}, \frac{1}{2})$, but at the zone boundary near $(\frac{1}{4}, \frac{1}{4})$ the "dispersion" becomes nearly vertical.

Constant momentum scans in Fig. 3 show that this vertical dispersion at the zone boundaries is due to the second short-lived and damped-in-energy component to the cross section. To fully separate these two components, we have fit energy scans to two harmonic oscillators, one being

resolution limited and the second damped in energy. The sharp component is denoted by the filled circles in Fig. 4(c). To extract an estimate for the localized J_{RKKY} exchange, we have fit the peak locations of the sharp component to the dispersion for $j_{\mathrm{eff}} = \frac{1}{2}$ spins (capturing the doublet nature of the ground state) on a square lattice. We have followed the classic model previously applied to Rb_2MnF_4, where a lattice periodic dispersion of $E(\vec{q}) = 2J_{\mathrm{RKKY}}\sqrt{\alpha^2 - \gamma(\vec{q})^2}$, with $\gamma(\vec{q}) = \cos[\pi(H+K)]\cos[\pi(-K+H)]$, was used. This provides a simple means of parametrizing the data and finding an estimate of the nearest-neighbor in-plane exchange. We note that this model does not capture the out-of-plane mode, which is found to show little dispersion and originates from weak coupling between the Ce^{3+} layers. Based on the fit in Fig. 4 to this parametrization, we extract $J_{\mathrm{RKKY}} = 0.88 \pm 0.05$ meV and an anisotropy $\alpha = 1.06 \pm 0.02$ meV.

Having described the sharp component sensitive to the antiferromagnetic exchange, we now discuss the broad continuum of scattering at higher energies. We interpret and describe this component in terms of a multimagnon model termed the "1 + 2" model. The heavily damped features originate from unstable particles, where energy and momentum conservation result in a decay process. As noted in Ref. [60], the presence of the three modes imposed by the helical structure implies that excitations can decay into lower-energy quasiparticles, assuming there is a binding interaction. For a given momentum transfer $\vec{k}$, the two-particle excitations form a continuum of states, and the energy and momentum positions where the cross section is finite are defined by conservation of momentum and energy. Following the classical theory outlined in Refs. [61,62] and using our parametrization of the single-magnon scattering, we have calculated the energy and momentum dependence of the allowed multimagnon scattering. Figure 4(d) shows a plot of the scaled calculation with the one-magnon term superimposed to give the sharp component. The momentum-integrated intensity from the calculations is overplotted in Fig. 4(b). Deviations from calculations at low energies are likely due to experimental limitations owing to resolution, incoherent nuclear scattering, and absorption.

Several features are reproduced in the multiparticle calculation: first, the broad continuum of scattering that extends up to nearly $2 \times J_{\mathrm{RKKY}}$; and second, the nearly vertical columns of scattering that extend up in energy near the zone boundary. Near the magnetic zone boundary, as illustrated in Fig. 3, the two components can be separated, with both accounting for roughly equal amounts in terms of the integrated intensity. The multiparticle model, therefore, provides an account of the neutron cross section once the single-magnon component is parameterized, giving the correct energy bandwidth and momentum dependence. The multiparticle continuum is also predicted to have a longitudinal polarization [47], consistent with the persistence to large L shown in Fig. 2.

One aspect that is not explicit in this analysis is how the coupling between single quasiparticles originates, and what determines the relative spectral weight between the single and multiparticle components. In insulating magnets, the spectral weight in the continuum comes from the Bragg peak; in $CeRhIn_5$, however, our analysis shows that the spectral weight draws from the inelastic component. The symmetry of the helical magnetic structure simply implies that such multiparticle scattering is allowed in the neutron scattering cross section. Such processes may be determined by cubic terms in the Hamiltonian, or possibly coupling resulting from the itinerant electronic nature of $CeRhIn_5$, as discussed elsewhere [63–66]. However, we note that in classical and insulating magnets the multiparticle continuum is weak, comprising ~1%–2% of the total spectral weight in Rb_2MnF_4 [61]. The relatively large size of the multiparticle continuum in $CeRhIn_5$ suggests that localized effects are not the cause, and that the itinerant properties are important. Our experiment suggests a low-energy scale in $CeRhIn_5$ where the single-quasiparticle description breaks down and interactions become important.

The physics here might be more general and, in particular, enhanced broadening in the neutron cross section has been observed near the zone boundary in metallic $Fe_{1+x}Te$ [67] and the cuprates $YBa_2Cu_3O_{6.35}$ [68,69], La_2CuO_4 [70], and $Sr_2CuO_2Cl_2$ [71]. These might indicate an interaction similar to that discussed here, yet much weaker due to symmetry constraints determined by the collinear structures. An alternate view is that the continuum in $CeRhIn_5$ results from the single-magnon branch at low energies interacting with a continuum of electronic excitations, as suggested in itinerant ferromagnets magnets such as MnSi [72] and Fe [73]. However, this scenario results in the disappearance or strong dampening of the single-magnon branch, and not the presence of two distinct components observed here in $CeRhIn_5$. This high-energy continuum may represent a direct measure of the hybridization gap that characterizes the energy scale where the quasiparticles cross over from localized to itinerant; such energy scales are expected to be on the order of ~meV in $CeRhIn_5$ [10].

In summary, we have studied the excitations in helical $CeRhIn_5$ and found the presence of a strong continuum along with sharp single-magnon excitations. Given that both components are required to satisfy neutron scattering sum rules, we understand the cross section in terms of a $1 + 2$ particle model, where the broad component originates from multiparticle states with the energy and momentum dependence fixed by energy and momentum conservation laws determined by the single-magnon cross section. We propose the multiparticle component originates from coupled magnons, observable given the relaxed symmetry constraints from a helical magnet. Our

measurements directly observe the breakdown of the single-quasiparticle, or single-magnon, picture for an itinerant magnet.

This work was funded by the Carnegie Trust for the Universities of Scotland, the Royal Society, the Royal Society of Edinburgh, the STFC, and the EPSRC (Grant No. EP/M01052X/1). Part of this work was carried out at the Brookhaven National Laboratory, which is operated for the U. S. Department of Energy by Brookhaven Science Associates (Grant No. DE-AcO2-98CH10886).

Note added.—After submission we became aware of Ref. [74] in which the low-energy magnetic fluctuations were studied. These results are in agreement with our "one-magnon" component; however, in addition to this we also report the multiparticle component at higher energies comprising significant spectral weight.

[1] P. W. Anderson, Science **235**, 1196 (1987).
[2] F. C. Zhang and T. M. Rice, Phys. Rev. B **37**, 3759(R) (1988).
[3] K. B. Efetov, H. Meier, and C. Pepin, Nat. Phys. **9**, 442 (2013).
[4] T. H. Hand, J. S. Helton, S. Y. Chu, D. G. Nocera, J. A. Rodriguez-Rivera, C. Broholm, and Y. S. Lee, Nature (London) **492**, 406 (2012).
[5] M. A. de Vries, J. R. Stewart, P. P. Deen, J. O. Piatek, G. J. Nilsen, H. M. Ronnow, and A. Harrison, Phys. Rev. Lett. **103**, 237201 (2009).
[6] P. Coleman, C. Pepin, Q. Si, and R. Ramazashvili, J. Phys. Condens. Matter **13**, R723 (2001).
[7] J. D. Thompson, R. Movshovich, Z. Fisk, F. Bouquet, N. J. Curro, R. A. Fisher, P. C. Hammel, H. Hegger, M. F. Hundley, M. Jaime, P. G. Pagliuso, C. Petrovic, N. E. Phillips, and J. L. Sarrao, J. Magn. Magn. Mater. **226–230**, 5 (2001).
[8] T. Park and J. D. Thompson, New J. Phys. **11**, 055062 (2009).
[9] J. Paglione, M. A. Tanatar, D. G. Hawthorn, R. W. Hill, F. Ronning, M. Sutherland, L. Taillefer, C. Petrovic, and P. C. Canfield, Phys. Rev. Lett. **94**, 216602 (2005).
[10] T. Park, M. J. Graf, L. Boulaevskii, J. L. Sarrao, and J. D. Thompson, Proc. Natl. Acad. Sci. U.S.A. **105**, 6825 (2008).
[11] M. Fujita, H. Hiraka, M. Matsuda, M. Matsuura, J. M. Tranquada, S. Wakimoto, G. Xu, and K. Yamada, J. Phys. Soc. Jpn. **81**, 011007 (2012).
[12] M. A. Kastner, R. J. Birgeneau, G. Shirane, and Y. Endoh, Rev. Mod. Phys. **70**, 897 (1998).
[13] R. J. Birgeneau, C. Stock, J. M. Tranquada, and K. Yamada, J. Phys. Soc. Jpn. **75**, 111003 (2006).
[14] C. Petrovic, R. Movshovich, M. Jaime, P. G. Pagliuso, M. F. Hundley, J. L. Sarrao, Z. Fisk, and J. D. Thompson, Europhys. Lett. **53**, 354 (2001).
[15] D. Hall, E. Palm, T. P. Murphy, S. W. Tozer, C. Petrovic, E. Miller-Ricci, L. Peabody, C. Q. H. Li, U. Alver, R. G. Goodrich, J. L. Sarrao, P. G. Pagliuso, J. M. Wills, and Z. Fisk, Phys. Rev. B **64**, 064506 (2001).
[16] G. R. Stewart, Rev. Mod. Phys. **83**, 1589 (2011).
[17] J. Paglione and R. L. Greene, Nat. Phys. **6**, 645 (2010).
[18] D. C. Johnston, Adv. Phys. **59**, 803 (2010).
[19] W. Bao, P. G. Pagliuso, J. L. Sarrao, J. D. Thompson, Z. Fisk, J. W. Lynn, and R. W. Erwin, Phys. Rev. B **62**, R14621 (2000).
[20] W. Bao, G. Aeppli, J. W. Lynn, P. G. Pagliuso, J. L. Sarrao, M. F. Hundley, J. D. Thompson, and Z. Fisk, Phys. Rev. B **65**, 100505(R) (2002).
[21] S. Raymond, E. Ressouche, G. Knebel, D. Aoki, and J. Flouquet, J. Phys. Condens. Matter **19**, 242204 (2007).
[22] G. F. Chen, K. Matsubayashi, S. Ban, K. Deguchi, and N. K. Sato, Phys. Rev. Lett. **97**, 017005 (2006).
[23] J. Paglione, P. C. Ho, M. B. Maple, M. A. Tanatar, L. Taillefer, Y. Lee, and C. Petrovic, Phys. Rev. B **77**, 100505(R) (2008).
[24] T. Park, V. A. Sidorov, F. Ronning, J. X. Zhu, Y. Tokiwa, H. Lee, E. D. Bauer, R. Movshovich, J. L. Sarrao, and J. D. Thompson, Nature (London) **456**, 366 (2008).
[25] T. Park, H. Lee, I. Martin, X. Lu, V. A. Sidorov, K. Gofryk, F. Ronning, E. D. Bauer, and J. D. Thompson, Phys. Rev. Lett. **108**, 077003 (2012).
[26] L. Mendonça Ferreira, T. Park, V. Sidorov, M. Nicklas, E. M. Bittar, R. Lora-Serrano, E. N. Hering, S. M. Ramos, M. B. Fontes, E. Baggio-Saitovich, H. Lee, J. L. Sarrao, J. D. Thompson, and P. G. Pagliuso, Phys. Rev. Lett. **101**, 017005 (2008).
[27] K. Izawa, H. Yamaguchi, Y. Matsuda, H. Shishido, R. Settai, and Y. Onuki, Phys. Rev. Lett. **87**, 057002 (2001).
[28] H. Aoki, T. Sakakibara, H. Shishido, R. Settai, Y. Onuki, P. Miranovic, and K. Machida, J. Phys. Condens. Matter **16**, L13 (2004).
[29] C. Stock, C. Broholm, Y. Zhao, F. Demmel, H. J. Kang, K. C. Rule, and C. Petrovic, Phys. Rev. Lett. **109**, 167207 (2012).
[30] C. Stock, C. Broholm, J. Hudis, H. J. Kang, and C. Petrovic, Phys. Rev. Lett. **100**, 087001 (2008).
[31] S. Raymond, K. Kaneko, A. Hiess, P. Steffens, and G. Lapertot, Phys. Rev. Lett. **109**, 237210 (2012).
[32] M. Kenzelmann, T. Strassle, C. Niedermayer, M. Sigrist, B. Padmanabham, M. Zolliker, A. D. Bianchi, R. Movshovich, E. D. Bauer, J. L. Sarrao, and J. D. Thompson, Science **321**, 1652 (2008).
[33] E. Blackburn, P. Das, M. R. Eskildsen, E. M. Forgan, M. Laver, C. Niedermayer, C. Petrovic, and J. S. White, Phys. Rev. Lett. **105**, 187001 (2010).
[34] J. A. Rodriguez, D. M. Adler, P. C. Brand, C. Broholm, J. C. Cook, C. Brocker, R. Hammond, Z. Huang, P. Hundertmakr, J. W. Lynn, N. C. Maliszewskyj, J. Moyer, J. Orndorff, D. Pierce, T. D. Pike, G. Scharfstein, S. A. Smee, and R. Vilaseca, Meas. Sci. Technol. **19**, 034023 (2008).
[35] V. F. Sears, Neutron News **3**, 26 (1992).
[36] B. J. Wuensch and C. T. Prewitt, Z. Kristallogr. **122**, 24 (1965).
[37] See Supplemental Material at http://link.aps.org/supplemental/10.1103/PhysRevLett.114.247005 for additional experimental information (including data access), discussion of the magnetic order parameter, a description of the crystal field scheme, and details regarding the absorption correction.

[38] F. Tasset, P. J. Brown, E. Lelievre-Berna, T. Roberts, S. Pujol, J. Allibon, and E. Bourgeat-Lami, Physica (Amsterdam) **267B–268B**, 69 (1999).
[39] M. Blume, Phys. Rev. **130**, 1670 (1963).
[40] P. J. Brown, J. B. Forsyth, and F. Tasset, Proc. R. Soc. A **442**, 147 (1993).
[41] M. T. Hutchings, Solid State Phys. **16**, 227 (1964).
[42] J. O. Dimmock, Phys. Rev. **130**, 1337 (1963).
[43] H. F. Franzen, Chem. Mater. **2**, 486 (1990).
[44] P. J. Brown, in *Mathematical, Physical and Chemical Tables*, International Tables of Crystallography Vol. C (Kluwer, Dordrecht, 2006).
[45] A. D. Christianson, J. M. Lawrence, P. G. Pagliuso, N. O. Moreno, J. L. Sarrao, J. D. Thompson, P. S. Riseborough, S. Kern, E. A. Goremychkin, and A. H. Lacerda, Phys. Rev. B **66**, 193102 (2002).
[46] T. Willers, Z. Hu, N. Hollmann, P. O. Korner, J. Gegner, T. Burnus, H. Fujiwara, A. Tanaka, D. Schmitz, H. H. Hsieh, H. J. Lin, C. T. Chen, E. D. Bauer, J. L. Sarrao, E. Goremychkin, M. Koza, L. H. Tjeng, and A. Severing, Phys. Rev. B **81**, 195114 (2010).
[47] M. E. Zhitomirsky and A. L. Chernyshev, Rev. Mod. Phys. **85**, 219 (2013).
[48] J. Villain, J. Physiol. **35**, 27 (1974).
[49] D. A. Tennant, T. G. Perring, R. A. Cowley, and S. E. Nagler, Phys. Rev. Lett. **70**, 4003 (1993).
[50] D. A. Tennant, R. A. Cowley, S. E. Nagler, and A. M. Tsvelik, Phys. Rev. B **52**, 13368 (1995).
[51] B. Lake, A. M. Tsvelik, S. Notbohm, D. A. Tennant, T. G. Perring, M. Reehuis, C. Sekar, G. Krabbes, and B. Buchner, Nat. Phys. **6**, 50 (2010).
[52] N. B. Christensen, H. M. Ronnow, D. F. McMorrow, A. Harrison, T. G. Perring, M. Enderle, R. Coldea, L. P. Regnault, and G. Aeppli, Proc. Natl. Acad. Sci. U.S.A **104**, 15264 (2007).
[53] M. B. Stone, I. A. Zaliznyak, T. Hong, C. L. Broholm, and D. H. Reich, Nature (London) **440**, 187 (2006).
[54] I. A. Zaliznyak, S. H. Lee, and S. V. Petrov, Phys. Rev. Lett. **87**, 017202 (2001).
[55] M. Kenzelmann, R. A. Cowley, W. J. L. Buyers, R. Coldea, J. S. Gardner, M. Enderle, D. F. McMorrow, and S. M. Bennington, Phys. Rev. Lett. **87**, 017201 (2001).
[56] A. V. Chubukov, J. Phys. C **17**, L991 (1984).
[57] C. Stock, L. C. Chapon, A. Schneidewind, Y. Su, P. G. Radaelli, D. F. McMorrow, A. Bombardi, N. Lee, and S. W. Cheong, Phys. Rev. B **83**, 104426 (2011).
[58] R. Coldea, D. A. Tennant, and Z. Tylczynski, Phys. Rev. B **68**, 134424 (2003).
[59] D. Dalidovich, R. Sknepnek, A. J. Berlinsky, J. Zhang, and C. Kallin, Phys. Rev. B **73**, 184403 (2006).
[60] A. L. Chernyshev and M. E. Zhitomirsky, Phys. Rev. Lett. **97**, 207202 (2006).
[61] T. Huberman, R. Coldea, R. A. Cowley, D. A. Tennant, R. L. Leheny, R. J. Christianson, and C. D. Frost, Phys. Rev. B **72**, 014413 (2005).
[62] I. U. Heilmann, J. K. Kjems, Y. Endoh, G. F. Reiter, G. Shirane, and R. J. Birgeneau, Phys. Rev. B **24**, 3939 (1981).
[63] A. H. MacDonald, S. M. Girvin, and D. Yoshioka, Phys. Rev. B **37**, 9753 (1988).
[64] A. W. Sandvik and R. R. P. Singh, Phys. Rev. Lett. **86**, 528 (2001).
[65] T. C. Hsu, Phys. Rev. B **41**, 11379 (1990).
[66] O. F. Syljuasen and P. A. Lee, Phys. Rev. Lett. **88**, 207207 (2002).
[67] C. Stock, E. E. Rodriguez, O. Sobolev, J. A. Rodriguez-Rivera, R. A. Ewings, J. W. Taylor, A. D. Christianson, and M. A. Green, Phys. Rev. B **90**, 121113(R) (2014).
[68] C. Stock, R. A. Cowley, W. J. L. Buyers, R. Coldea, C. L. Broholm, C. D. Frost, R. J. Birgeneau, R. Liang, D. Bonn, and W. N. Hardy, Phys. Rev. B **75**, 172510 (2007).
[69] C. Stock, R. A. Cowley, W. J. L. Buyers, C. D. Frost, J. W. Taylor, D. Peets, R. Liang, D. Bonn, and W. N. Hardy, Phys. Rev. B **82**, 174505 (2010).
[70] N. S. Headings, S. M. Hayden, R. Coldea, and T. G. Perring, Phys. Rev. Lett. **105**, 247001 (2010).
[71] K. W. Plumb, A. T. Savici, G. E. Granroth, F. C. Chou, and Y. J. Kim, Phys. Rev. B **89**, 180410(R) (2014).
[72] Y. Ishikawa, Y. Noda, Y. J. Uemura, C. F. Majkrzak, and G. Shirane, Phys. Rev. B **31**, 5884 (1985).
[73] D. M. Paul, P. W. Mitchell, H. A. Mook, and U. Steigenberger, Phys. Rev. B **38**, 580 (1988).
[74] P. Das, S.-Z. Lin, N. J. Ghimire, K. Huang, F. Ronning, E. D. Bauer, J. D. Thompson, C. D. Batista, G. Ehlers, and M. Janoschek, Phys. Rev. Lett. **113**, 246403 (2014).